Real-Time *In Situ* HRTEM-Resolved Resistance Switching of Ag_2S Nanoscale Ionic Conductor

Zhi Xu,[†,‡] Yoshio Bando,[†] Wenlong Wang,[‡] Xuedong Bai,[‡,*] and Dmitri Golberg[†,*]

[†]International Center for Materials Nanoarchitectonics (MANA), National Institute for Materials Science (NIMS), 1-1 Namiki, Tsukuba, Ibaraki 305-0044, Japan, and
[‡]Beijing National Laboratory for Condensed Matter Physics, Institute of Physics, Chinese Academy of Sciences, Beijing 100190, China

ARTICLE

ABSTRACT The switching behaviors of ionic/electronic mixed conductor-based solid electrolyte nonvolatile memories have been attributed to repetitive formation and breakage of the conductive pathways inside a solid electrolyte. However, direct evidence of such pathway existences and their formations has never been provided. Herein, we reproduced the switching behavior of a $Ag/Ag_2S/W$ sandwich structure inside a high-resolution transmission electron microscope equipped with a scanning tunneling microscope unit. The on/off current ratio of 5 orders of magnitude was documented. The *in situ* formation and breakage of a nanoscale conductive channel were ultimately verified in real time and under atomic resolution. We found that a conducting Ag_2S argentite phase and a Ag nanocrystal together formed the ionic and electronic conductive channel. The preferential atomic sites for Ag nanocrystal growth within the argentite phase were finally clarified.

KEYWORDS: silver sulfide · ionic conductors · high-resolution transmission electron microscopy · resistance nanoswitch · nonvolatile memory

Along with the development of microelectronics, research on low-power, low-cost, and high-density memory devices is required in order to design novel portable digital systems. Extensive research has been conducted to find switches that can replace those made using conventional Si-based technologies. Ionic and electronic mixed conductor-based solid electrolyte nonvolatile memories have attracted a great deal of attention.[1−3] Filamentary switching mechanism has widely been accepted; that is, the switching behavior is attributed to repetitive formation and breakage of the conductive filament inside a solid electrolyte. Although some experiments[4−6] and theoretical works[7−9] have been performed in an attempt to elucidate the formation mechanism of such metallic filaments, neither the direct evidence of such pathways nor their formation details have been provided. Furthermore, it is not clear how a filament grows microscopically and how the sulfide lattice responds. Herein, we entirely reproduced the switching behavior of a $Ag/Ag_2S/W$ sandwich structure inside a high-resolution transmission electron microscope (HRTEM) equipped with a scanning tunneling microscope (STM) unit. Through these direct experiments, the chemical composition and crystal structure of the initial state (*i.e.*, the off-state) and the conducting state (*i.e.*, the on-state) were carefully analyzed using in-tandem spatially resolved energy-dispersive X-ray spectroscopy (EDS) and HRTEM lattice imaging. The conductive nanoscale pathway was indeed directly imaged under the atomic resolution (~1.7 Å). On the basis of the observations, a refined switching model of a Ag_2S-based nonvolatile memory nanodevice was proposed.

RESULTS AND DISCUSSION

The basic experiment configuration is shown in Figure 1a. Note that, during the experiments, the W tip was grounded, so that a positive bias sign means that the Ag electrode is positively biased.

When we continuously swept a bias voltage from 0 mV → 200 mV → 0 mV → −300 mV → 0 mV, a very clear bipolar switching $I-V$ curve was recorded (Figure 1d). At the beginning, the current is very low. By sweeping the bias to positive values, the conductance suddenly increases at 130 mV, and the nanodevice transforms to the on-state. Subsequent sweeping of the bias back to negative values suddenly decreases the conductance at −145 mV, and the device goes into the off-state. As indicated in the logarithmic scale plot of the positive bias range (the inset in Figure 1d), the on/off ratio is larger than 5 orders of magnitude. Such conductance switching was repeatable, and the on/off states persisted when the applied bias was lower than the threshold voltage. During voltage scanning, the corresponding morphology changes were noticed in the Ag_2S part. When the

*Address correspondence to xdbai@aphy.iphy.ac.cn, golberg.dmitri@nims.go.jp.

Received for review March 10, 2010 and accepted April 09, 2010.

Published online April 16, 2010.
10.1021/nn100483a

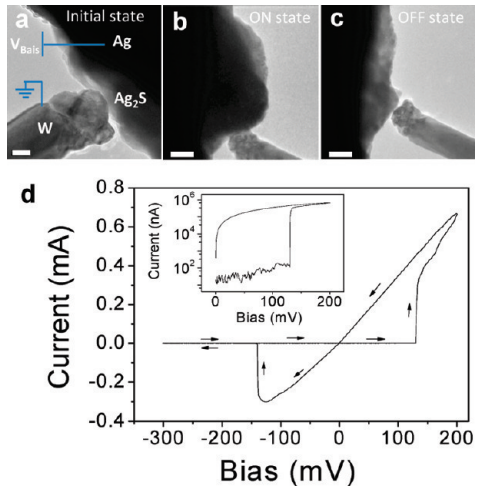

Figure 1. (a) Low-magnification TEM image corresponding to the initial off-state of a Ag_2S-based ionic resistance nanoswitch. The experimental electrical circuit scheme is added. Scale bar = 20 nm. (b) Low-magnification TEM image corresponding to the on-state of the device. A newly grown nanocrystal is seen. Scale bar = 50 nm. (c) Low-magnification TEM image corresponding to the off-state. The grown crystal shrank back. Scale bar = 50 nm. (d) Dual sweep scan *I*−*V* curve of this device. Inset: *I*−*V* curve (positive range) in the logarithmic scale. The 5 orders of magnitude on/off current change is documented.

current suddenly increased (off-to-on transition), a piece of some new nanocrystal was seen to grow (Figure 1b). This crystal kept its shape until the current suddenly dropped (on-to-off transition), then it shrank back immediately (Figure 1c). This morphology change repeatedly took place in parallel with the on/off switching cycles (see movie 1 in the Supporting Information).

We then carefully examined the crystal structures peculiar to different states. For the starting Ag_2S (Figure 2), the EDS analyses showed that the atomic ratio of Ag to S was close to 2. On the HRTEM images, we could only find nanocrystals of the nonconducting acanthite Ag_2S phase. Thus, we confirmed that the as-grown Ag_2S was in the semiconducting acanthite phase (monoclinic structure) having a 1.2 eV band gap.[10] Diffusion of Ag cations in this phase is hampered,[10,11] so the device was not initially conductive.

Once we applied a positive bias pulse, we kept the device in its on-state, and some crystal grew from the Ag_2S base and its tip touched the tungsten tip, forming a triangle-like morphological domain (Figure 3). First, we carried out the nanoprobe EDS analyses in different regions of this triangular crystal. Its end (close to the W tip) showed a very high atomic ratio of Ag to S, which was 11.1. This ratio dropped in the regions far away from the W tip (Figure 3a,b1−b3), but it was still larger than 2. This means that this newly grown nanocrystal is Ag-rich. Then we took HRTEM images from the particular areas where the EDS spectra were captured. In the tip area, almost pure Ag single crystal was found. In the intermediate area, we could find both a Ag single crystal and the argentite phase Ag_2S. The conductivity

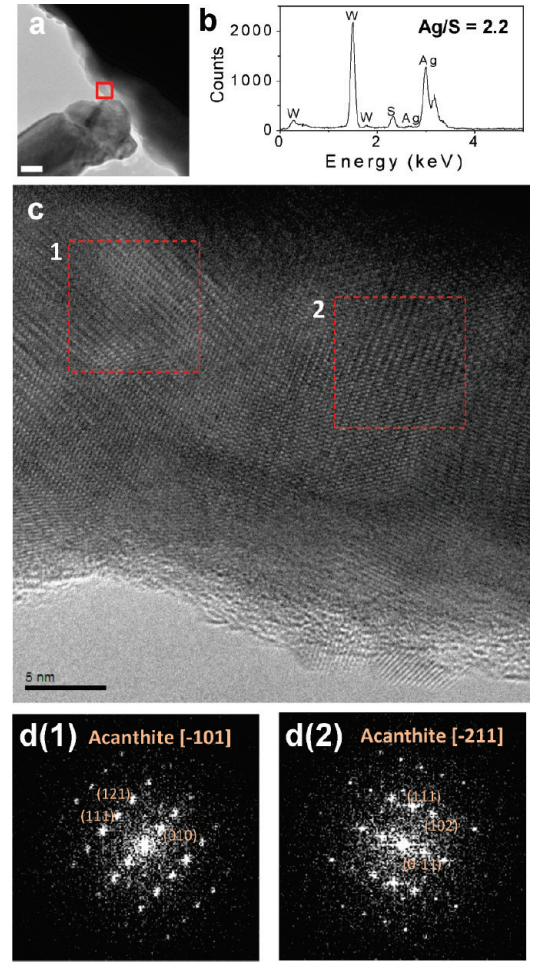

Figure 2. (a) Low-magnification TEM image corresponding to the initial off-state. Scale bar = 20 nm. (b) EDS spectrum taken in the framed area in (a). The atomic ratio of Ag to S is about 2.2. (c) High-magnification TEM image of the framed area marked in (a). (d1) FFT pattern of the area #1 marked in (c). Analysis of this FFT pattern implies that the area represents the acanthite Ag_2S phase viewed along the [−101] zone axis. (d2) FFT pattern of the area #2 marked in (c). Identification of this FFT pattern shows that the area represents the acanthite Ag_2S phase viewed along the [−211] zone axis.

of silver is 6.3×10^5 1/Ωcm, that of the argentite phase is about 1.6×10^3 1/Ωcm.[10] For the acanthite phase, it is only 2.5×10^{-3} 1/Ωcm[10] at room temperature, that is 6 orders of magnitude lower than for the argentite phase. It is thus reasonable to conclude that the conducting channel is made of a mixture of silver and the argentite Ag_2S.

Then, a negative bias was applied to the device in order to turn it off. We saw that the regarded crystal shrank backward. The EDS result indicated that the atomic ratio of Ag to S became 1.8 in the remaining materials. Fast Fourier transform (FFT) analysis of the HRTEM image showed that it corresponded to the pure nonconductive acanthite phase (Figure 4).

Silver sulfide is easy to decompose under electron-beam irradiation. To minimize the irradiation effects, we used the minimum condenser lens aperture, which

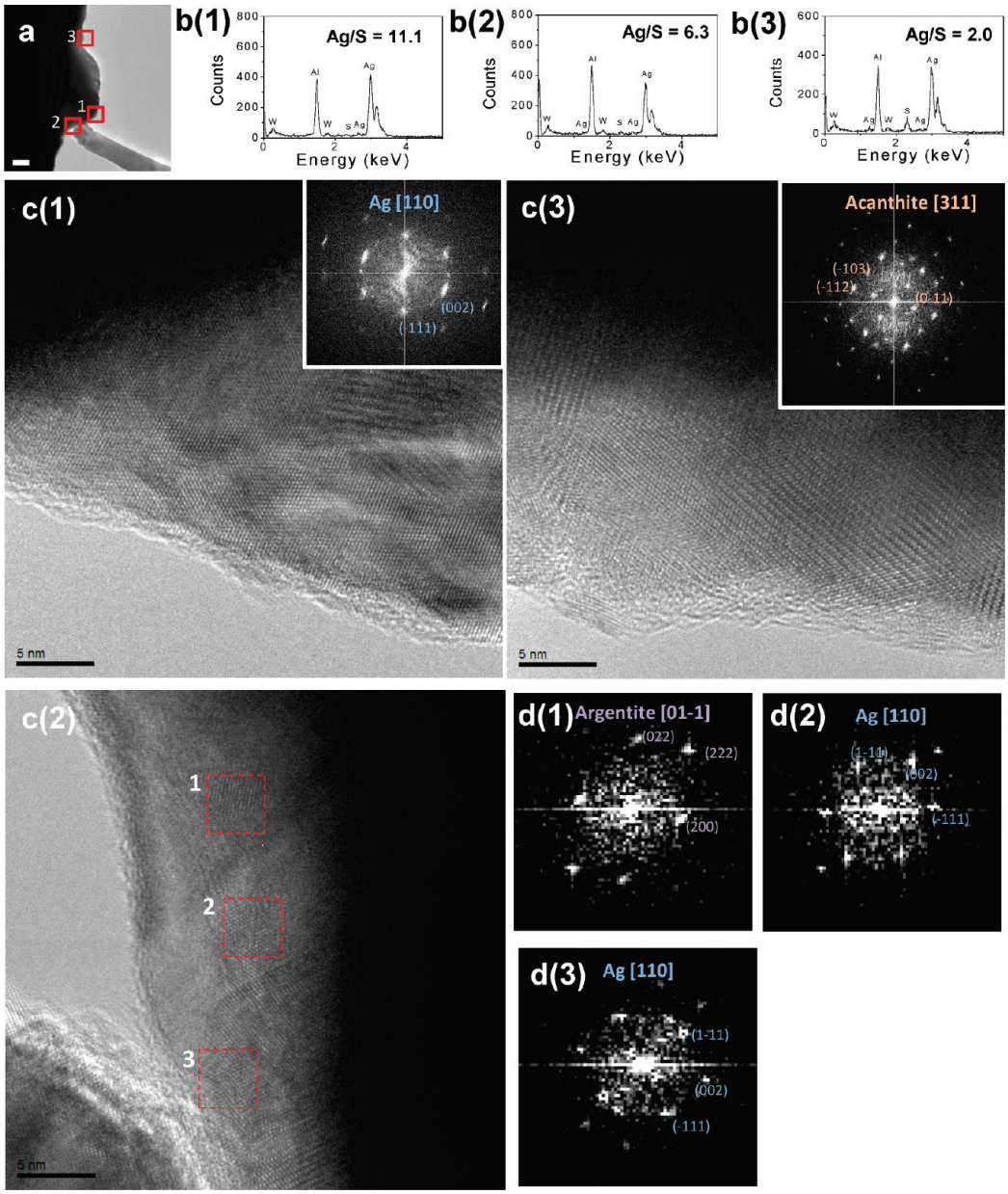

Figure 3. (a) Low-magnification TEM image corresponding to the on-state of a nanodevice. Scale bar = 50 nm. (b1−b3) EDS spectra taken in the framed areas #1−#3 in (a). The atomic ratios of Ag to S in these areas are 11.1, 6.3, and 2.0, respectively. (c1) High-magnification TEM image of the area #1 marked in (a). Inset: FFT pattern of this HRTEM image revealing the pure Ag phase viewed along the [110] zone axis. (c2) High-magnification TEM image of the framed area #2 marked in (a). (c3) High-magnification TEM image of the framed area #3 in (a). Inset: FFT pattern of this HRTEM image displaying the pure acanthite phase projected along the [311] zone axis. (d1−d3) FFT patterns of the areas #1−#3 framed in (b2). The identification shows that area #1 is in the argentite phase, whereas areas #2 and #3 consist of pure Ag.

results in quite low illumination brightness (1−2 A/cm^2) under TEM observations. We did not see any structure change during long-time high-resolution observations. Moreover, we have compared the switching process under both beam-on and beam-off conditions. In the beam-on regime, the electron beam was always on. For beam-off conditions, the electron beam was blanked when a voltage bias was applied (at that time, the redox process and morphology change actually occurred). The on- and off-states under these two conditions showed no difference. On the basis of the above two observations, we believe that the electron-beam irradiation effect can be neglected in our experiments.

In order to have further insights into the switching processes, we selected a very thin and narrow area where we could see lattice resolution of the switch structure as a whole (Figure 5a,b). When this domain was turned on, very clear new lattice fringes appeared in area #3, as marked in Figure 5b (see a real-time movie in the Supporting Information). Detailed FFT analyses of these lattices fringes are presented in Figure 5c,d. The area #1 almost did not change, being kept in the

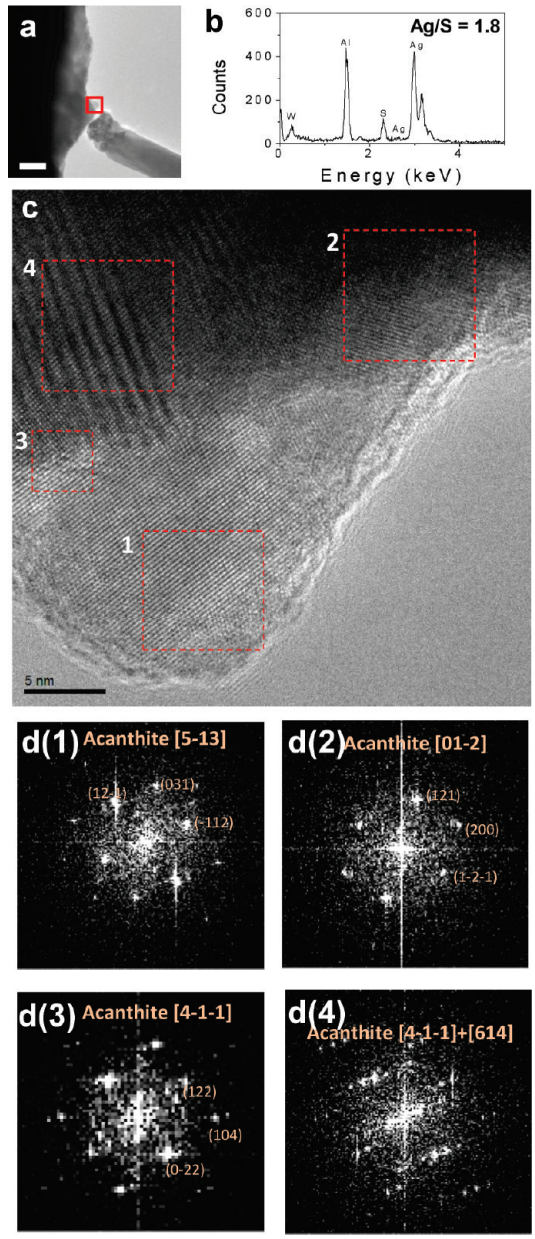

Figure 4. (a) Low-magnification TEM image corresponding to the off-state of a nanodevice. Scale bar = 50 nm. (b) EDS analysis of the area framed in (a). Quantitative analysis gives the atomic ratio of Ag to S of 1.8 in this area. (c) HRTEM image of the area framed in (a). (d1−d4) FFT images of areas #1−#4 framed in (c). They are all in the acanthite phase.

acanthite phase. In area #2, the argentite (002) fringes appeared. In area #3, both argentite and pure Ag fringes appeared. In area #4, we saw the argentite (002) fringes for the both on- and off-states, but the contrast and intensity of these fringes increased for the on-state. Apart from these numbered areas, on the left-hand-side of this long and narrow rod, we could see that the vertical argentite (002) fringes appeared for the on-state. These observations and analyses confirmed our statement that the pure Ag and argentite Ag_2S phase together had formed the regarded conducting channel. We then used FFT filtering together with the inversed FFTs to extract a certain phase for the on- and off-state HRTEM images, so that we could see how and where these phase transitions and crystal growth took place. The results are illustrated in Figure 5e (for the off-state) and in Figure 5f (for the on-state) in sequence for the acanthite, argentite, Ag, and an overlay of the two conductive phases (*i.e.*, Ag + argentite). It is evident that (i) a part of the acanthite phase transformed into the argentite phase at the top right corner of the most left images; (ii) the argentite phase grew bigger in the middle, left edge, and the bottom parts of the images; (iii) excessive Ag accumulated and formed a Ag nanocrystal surrounded by the argentite phase in the middle image part. The total conducting channel (from top to bottom) is clearly seen in the most right image in Figure 5f. Some small pieces of the argentite phase also exist outside of this channel; they may also partially contribute to the conductance.

Normally, acanthite is stable below 178 °C. When temperature is higher than 178 °C, Ag_2S transforms into argentite.[12] Conductivity of acanthite is quite low; however, argentite has a metallic behavior.[12] In our experiments, we found that this transition took place at room temperature and only within a conductive pathway. The argentite not only forms the parts of the conducting channel but also provides the pathway for the Ag cations' migration. In fact, the Ag cations can only migrate in the argentite but not in the acanthite Ag_2S phase. Since it has been demonstrated that an electrical field can decrease the phase transformation temperature in various materials,[14−17] we think that such field, as well as the movement of Ag cations, induced this transition. The Joule heating effect may be excluded because the current is quite low at the off-state. The Ag-rich environment may help the high-temperature phase to survive at room temperature. In fact, it was confirmed that the argentite phase could exist in a Ag-rich environment at room temperature.[5]

On the basis of the present experimental observations and analyses, the total process of the resistance switching of a nanoscale Ag_2S-based superionic conductor is fully understood as follows. Initially, Ag_2S is in the acanthite nonconductive phase (Figure 6a). When a bias is applied, the Ag cations start to migrate, at the same time the acanthite phase transforms into the argentite one. The silver cations can be reduced anywhere along their migration way, but their reduction occurs mostly at the interface between the Ag_2S electrolyte and the cathode. The Ag atoms in the silver electrode are ionized and dissolved into Ag_2S to supply Ag cations. Due to Ag mass transport, the volume of Ag_2S electrolyte within the conducting channel increases, and the mixture of Ag and argentite grows on the original acanthite surface (Figure 6b). The pure Ag crystal starts to grow, while more and more acanthite Ag_2S transforms into argentite Ag_2S. A sudden resistance drop occurs when the conducting nanochannel en-

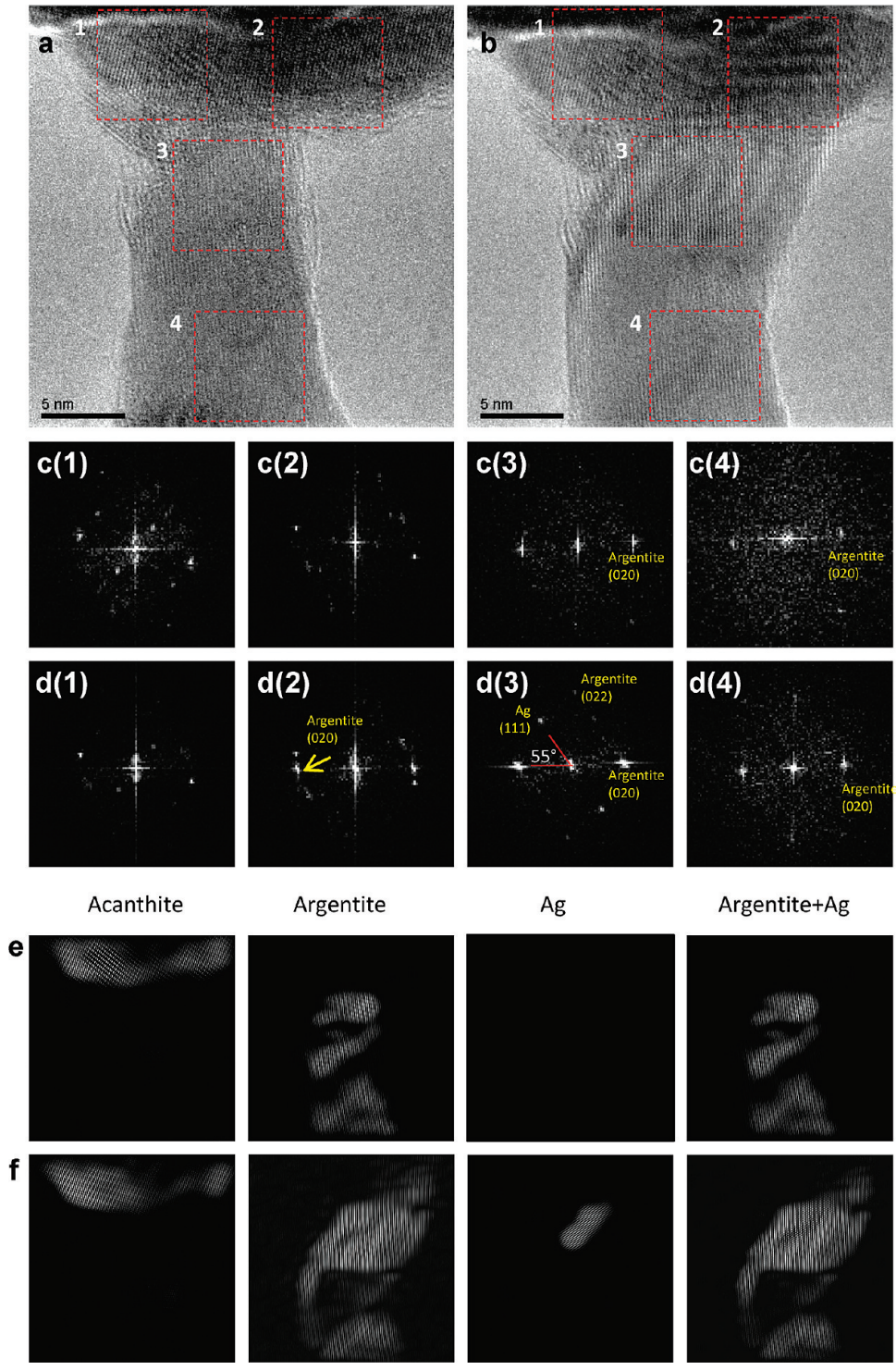

Figure 5. (a,b) Off- and on-states of a narrow and thin Ag_2S device region. The Ag electrode is located on the top part of the image; W electrode is in the bottom part. (c1−c4,d1−d4) FFT patterns of the areas from #1 to #4 framed in (a) and (b), respectively. When the device is switched from the off- to on-states, a FFT of area #1 has almost no change, the argentite (020) spot appears in area #2, the argentite (022) and Ag (111) spots appear in area #3, no new spots are seen in area #4, but the intensity of the argentite (020) reflection increases. (e,f) Individual phase images of the off- and on-states retrieved using the FFT filtering method. No Ag phase is visible for the off-state, so the phase map is totally black. The two conductive phases, *i.e.*, argentite Ag_2S and Ag, are added, as shown in the most right column.

tirely connects two electrodes (Figure 6c). After applying a negative bias, the Ag crystal starts to be ionized and Ag cations move toward the anode (Figure 6d). When the Ag-rich environment disappears, the argentite phase transforms back to the acanthite phase. Once the argentite Ag_2S + Ag conducting channel becomes trespassed by the nonconductive acanthite phase, the channel breaks, the resistance dramatically increases,

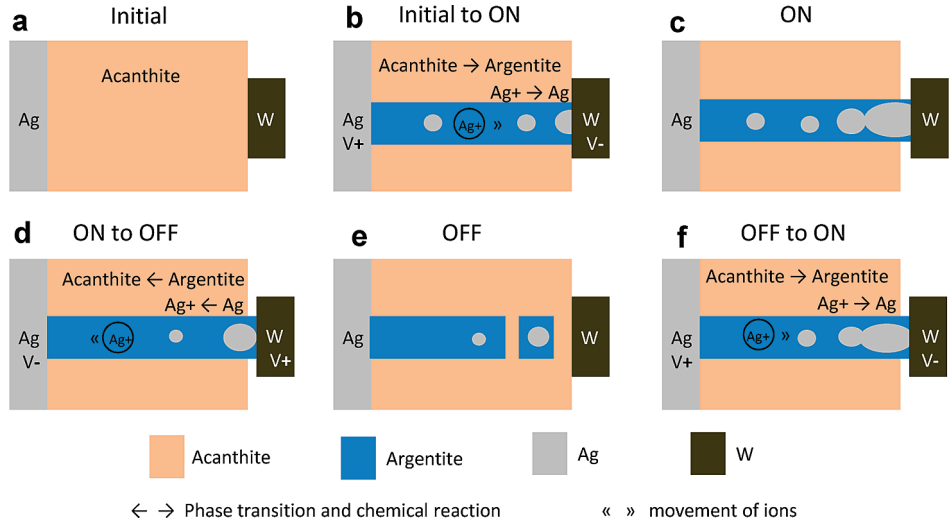

Figure 6. Schematics of an overall Ag_2S switch performance. (a) Initially, Ag_2S is in the nonconducting acanthite phase. (b) When a positive bias is applied, Ag cations start to migrate toward the cathode and are reduced to Ag atoms during their transport; the acanthite phase transforms into the argentite phase. (c) Continuous conducting channel made of argentite and Ag is built. Because a volume expands, the conducting mixture can grow out of the Ag_2S electrolyte. (d) When a negative bias is applied, the Ag crystal dissolves into the argentite phase, Ag cations migrate toward the anode, the argentite phase back-transforms into the acanthite phase. (e) When the conducting channel is trespassed by the nonconductive acanthite phase, the device is turned off. The conducting mixture shrinks back. (f) When a positive bias is applied again, the broken conductive channel is rebuilt due to the argentite phase and Ag formation.

and the whole device is turned off. Some argentite and Ag nanocrystals can also survive in the off-state since now Ag cations stop moving and the Ag-rich environment is maintained locally (Figure 6e). Once again, when a positive bias is applied, the conducting channel starts to rebuild itself; this time it only needs to restructure a nonconductive acanthite gap between the different conductive domains (Figure 6f).

In the argentite phase, the S anions form a rigid body-centered cubic lattice with Ag cations randomly occupying 1/3 of the 12d sites in the lattice (Wyckoff symbols; see ref 18; a 3D argentite unit cell is shown in the inset of Figure 7e). Calculations show the minimum energy barrier of 89 meV for a Ag cation jumping from one atomic site to another.[6] This result is basically consistent with our observations that the switching occurs at a bias of 130 meV. We never observed switching below 100 meV. The Ag(111) plane is the most close-packed plane of Ag (in area #3 in Figure 5b). During the HRTEM imaging, we detected the argentite (020)

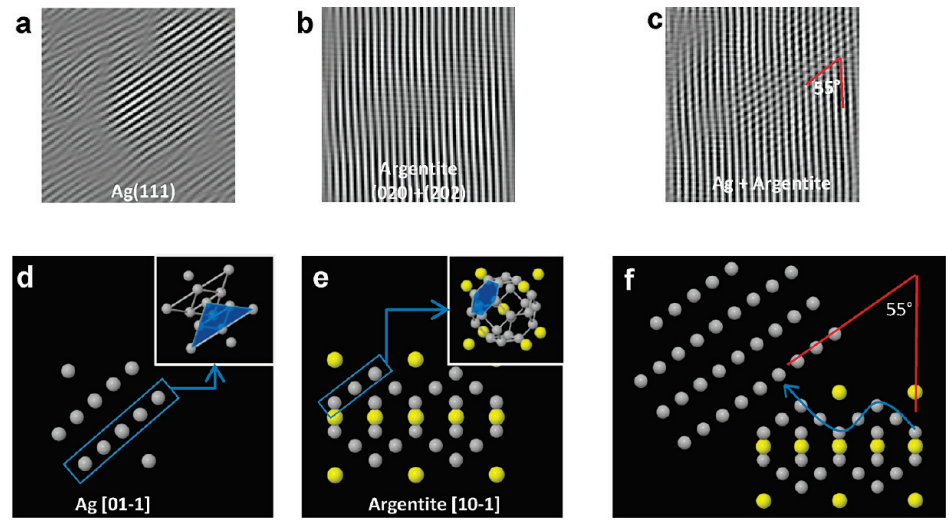

Figure 7. (a) Ag lattice-resolved image extracted from area #3 in Figure 5b. (b) Argentite phase image extracted from area #3 in Figure 5b. (c) Overlay of (a) and (b) which can be considered as a noise-reduced image of area #3 in Figure 5b. (d) Atomic model of Ag viewed along the [01−1] direction. A 3D unit cell with the marked plane of interest is shown in the top right corner inset. (e) Atomic model of an argentite Ag_2S phase viewed along the [10−1] direction. A 3D unit cell with the marked hexagonal plane at the 12d position is shown in the top right corner inset. (f) Atomic model revealing the orientation relationship between Ag and argentite. The Ag(111) plane is parallel to the hexagonal plane at the 12d position in argentite. A possible migration pathway of Ag ions is drawn. An angle between the Ag(111) and argentite (020) planes is ~55°, which is consistent with the experimental observations in Figure 5d3 and Figure 7c.

and (202) planes. This means that the argentite phase is viewed along its [10−1] zone axis. If we merge the atomic models of Ag and argentite Ag_2S together, we can see that the Ag (111) plane is parallel to one plane at the 12d position. In this configuration, the angle between the Ag(111) and argentite (020) planes is about 55°, which coincides with the experimental observations in Figure 5d3 and Figure 7c. The Ag atoms on the Ag(111) plane are arranged in a hexagonal fashion. The atomic plane at the 12d position of argentite also has a hexagonal symmetry. The two planes have the minimal lattice mismatch. Therefore, it is reasonable to assume that, when the Ag cations are reduced, the Ag atoms preferentially grow on the basis of this plane. Since Ag cations can migrate nearly freely between the 12d positions, we propose a possible migration pathway of Ag cations in Figure 7f.

CONCLUSION

In summary, for the first time, we have directly observed at the atomic resolution the formation and breakage of a conducting pathway in a superionic solid electrolyte resistance nanoswitch by complete reproducing of its performance inside the high-resolution transmission electron microscope equipped with the STM unit. In the particular case of Ag_2S, a conducting channel is created by the conducting Ag_2S argentite phase and the pure Ag crystal together. The Ag cations' migration pathway and the prime state of the Ag nanocrystal growth have also been clarified.

In the end, we would like to emphasize the two key points of this work that should draw the prime attention. First, a transformation from the acanthite to argentite Ag_2S plays the crucial role in the switching of a Ag_2S metal−insulator−metal (MIM) structure. Although this phase transformation has been known for more than 80 years, it has not been given full attention while considering the working principle of a Ag_2S MIM switch. Second, when the Ag atoms from a Ag electrode are dissolved into a Ag_2S electrolyte, and then reduced, the volume of the intermediate layer increases, so that a mixture of Ag and the argentite phase can grow out of the original surface of the electrolyte. This phenomenon was observed before but was not deeply addressed.[3−5,13] If a bias voltage is kept, the growth of a Ag crystal at the cathode will continue, as the Ag atoms from the Ag electrode are transported to the cathode, and the structure of a device could be totally damaged. If the two electrodes are firm and rigid, a mixture of the conducting phases may be confined, but surely, there will be a large strain level inside the device structure. This effect is destructive for the stable device performance and should be very carefully treated under its design. However, this detrimental effect could be minimized by precisely controlling the width and height of a turn-on voltage pulse.

Although the basic working principle of a Ag_2S atomic switch has properly been revealed in previous publications,[3−5,13] the present *real-time*, *in situ*, *atomic-resolution* work should be highly beneficial for the practical development of these advanced metal-cation-type nonvolatile memory devices. Besides Ag_2S (and the similar systems, Cu_2S[19] and Ag_2Se[20]), there are many other materials that show reversible resistance switching behavior, for example, $(Pr,Ca)MnO_3$,[21] $SrTiO_3$,[22] Ta_2O_5,[23] VO_2,[24] and TiO_2.[25] The detailed mechanisms of their functioning have not yet been decently elucidated due to a limited number of reliable experimental techniques and observations and theoretical calculations. The experiments designed and described in this contribution provide a general method to answer all sorts of fundamental questions related to the switch operations and should give inspiration to the whole field.

EXPERIMENTAL METHODS

To synthesize silver sulfide, a Ag wire (diameter = 0.5 mm, 99.9%, purchased from the Sigma-Aldrich Company) was loaded in a small quartz tube together with a sulfur powder (99.98%, purchased from the same company). This small quartz tube was evacuated to 10^{-3} Pa and then was sealed. The sealed quartz tube was heated to 200 °C for 30 min in a horizontal furnace. After that, it was broken and the sulfidized Ag wire was taken out. Then, the sulfidized Ag wire was annealed in argon (300 sccm) at ambient pressure at 200 °C for 30 min. We used a "Nanofactory Instruments" STM−TEM joint instrument inserted into a 300 kV JEM-3100FEF (JEOL, Omega Filter) field-emission high-resolution TEM. A sharp tungsten STM tip was fixed on the movable end of a piezotube. We delicately scratched the sulfidized Ag wire using another polished Ag wire, so that some small pieces of silver sulfide were transferred to it. The Ag wire with the Ag_2S tip-end was mounted in the HRTEM opposite the STM tungsten tip. Then we located a thin Ag_2S/Ag area in which we were able to see high-resolution lattice images, moved the W tip toward it, and made a physical contact. During the experiments, the W tip was grounded; bias voltage was applied on the Ag electrode.

Acknowledgment. This work was supported by the International Center for Materials Nanoarchitectonics (MANA) tenable at the National Institute for Materials Science, Japan, and the NSF (Nos. 50725209 and 10874218) and MOST (No. 2007CB936203) of China.

Supporting Information Available: Movie 1 shows the repetitive switching as well as the growth and disappearance of a solid Ag_2S + Ag nanocrystal electrolyte. Movie 2 presents the HRTEM real-time video corresponding to Figure 5. This material is available free of charge *via* the Internet at http://pubs.acs.org.

REFERENCES AND NOTES

1. Waser, R.; Aono, M. Nanoionics-Based Resistive Switching Memories. *Nat. Mater.* **2007**, *6*, 833–840.
2. Sawa, A. Resistive Switching in Transition Metal Oxides. *Mater. Today* **2008**, *11*, 28–33.
3. Terabe, K.; Hasegawa, T.; Nakayama, T.; Aono, M. Quantized Conductance Atomic Switch. *Nature* **2005**, *433*, 47–50.

4. Liang, C. H.; Terabe, K.; Hasegawa, T.; Negishi, R.; Tamura, T.; Aono, M. Ionic-Electronic Conductor Nanostructures Template-Confined Growth and Nonlinear Electrical Transport. *Small* **2005**, *1*, 971–975.
5. Kundu, M.; Terabe, K.; Hasegawa, T.; Aono, M. Effect of Sulfurization Conditions and Post-Deposition Annealing Treatment on Structural and Electrical Properties of Silver Sulfide Films. *J. Appl. Phys.* **2006**, *99*, 103501.
6. Morales-Masis, M.; Molen, S. J.; Fu, W. T.; Hesselberth, M. B.; Ruitenbeek, J. M. Conductance Switching in Ag_2S Devices Fabricated by *In Situ* Sulfurization. *Nanotechnology* **2009**, *20*, 095710.
7. Wang, Z.; Gu, T.; Tada, T.; Watanabe, S. Excess-Silver-Induced Bridge Formation in a Silver Sulfide Atomic Switch. *Appl. Phys. Lett.* **2008**, *93*, 152106.
8. Sun, S.; Xia, D. An *Ab-Initio* Calculation Study on the Super Ionic Conductors α-AgI and Ag_2X (X = S; Se) with bcc Structure. *Solid State Ionics* **2008**, *179*, 2330–2334.
9. Wang, Z.; Kadohira, T.; Tada, T.; Wataabe, S. Nonequilibrium Quantum Transport Properties of a Silver Atomic Switch. *Nano Lett.* **2007**, *7*, 2688–2692.
10. Junod, P.; Hediger, H.; Kilchor, B.; Wullschleger, J. Metal-Non-Metal Transition in Silver Chalcogenides. *Philos. Mag.* **1977**, *36*, 941–958.
11. Allen, R. L.; Moore, W. J. Diffusion of Silver in Silver Sulfide. *J. Phys. Chem.* **1959**, *63*, 223–226.
12. Emmons, R. C.; Stockwell, C. H.; Jones, R. H. B. Argentite and Acanthite. *Am. Mineral.* **1926**, *11*, 326–328.
13. Terabe, K.; Nakayama, T.; Hasegawa, T.; Aono, M. Ionic Electronic Cixed Conductor Tip of a Scanning Tunneling Microscope as a Metal Atom Source for Nanostructuring. *Appl. Phys. Lett.* **2002**, *80*, 4009–4011.
14. Li, Z.; Xu, Z.; Xi, Z.; Yao, X. Dielectric Response of PMN-0.32PT Single Crystal and Ceramics under DC Electric Field. *Ceram. Int.* **2004**, *30*, 2015–2018.
15. Bobnar, V.; Kutnjak, Z.; Pirc, R.; Levstik, A. Electric-Field−Temperature Phase Diagram of the Relaxor Ferroelectric Lanthanum-Modified Lead Zirconate Titanate. *Phys. Rev. B* **1999**, *60*, 6420–6427.
16. Zhao, X.; Tan, X.; Bokov, A. A.; Ye, Z.-G. Electric Field-Induced Phase Transitions in (111)-, (110)-, and (100)-Oriented $Pb(Mg_{1/3}Nb_{2/3})O_3$ Single Crystals. *Phys. Rev. B* **2007**, *75*, 104106.
17. Kim, H.; Chae, B.; Youn, D.; Kim, G.; Kang, K. Raman Study of Electric-Field-Induced First-Order Metal-Insulator Transition in VO_2-Based Devices. *Appl. Phys. Lett.* **2005**, *86*, 242101.
18. Wondratschek, H. *International Tables for Crystallography*, 5th ed.; Springer: The Netherlands, 2002; Vol. A, Chapter 8.3, pp 732−734.
19. Sakamoto, T.; Sunamura, H.; Kawaura, H.; Hasegawa, T.; Nakayama, T.; Aono, M. Nanometer-Scale Switches Using Copper Sulfide. *Appl. Phys. Lett.* **2003**, *82*, 3032–3034.
20. Schoen, D. T.; Xie, C.; Cui, Y. Electrical Switching and Phase Transformation in Silver Selenide Nanowires. *J. Am. Chem. Soc.* **2007**, *129*, 4116–4117.
21. Asamitsu, A.; Tomioka, Y.; Kuwahara, H.; Tokura, Y. Current Switching of Resistive States in Magnetoresistive Manganites. *Nature* **1997**, *388*, 50–52.
22. Meijer, G. I.; Staub, U.; Janousch, M.; Johnson, S. L.; Delley, B.; Neisius, T. Valence States of Cr and the Insulator-to-Metal Transition in Cr-Doped $SrTiO_3$. *Phys. Rev. B* **2005**, *72*, 155102.
23. Pinto, R. Filamentary Switching and Memory Action in Thin Anodic Oxides. *Phys. Lett. A* **1971**, *35*, 155–156.
24. Beaulieu, R. P.; Sulway, D. V.; Cox, C. D. Memory Properties of CdSe Single Crystals. *Solid-State Electron.* **1973**, *16*, 428–429.
25. Choi, B. J.; Jeong, D. S.; Kim, S. K. Resistive Switching Mechanism of TiO_2 Thin Films Grown by Atomic-Layer Deposition. *J. Appl. Phys.* **2005**, *98*, 033715.